Supplementary Information

Equatorial Coordination Optimization for Enhanced Axiality of Mononuclear Dy(III) Single-Molecule Magnets

Ke-Xin Yu, You-Song Ding, Yuan-Qi Zhai, Tian Han,* and Yan-Zhen Zheng*

[a] *Frontier Institute of Science and Technology (FIST), School of Science, Research Institute of Xi'an Jiaotong University (Zhejiang), State Key Laboratory of Mechanical Behavior for Materials, MOE Key Laboratory for Nonequilibrium Synthesis of Condensed Matter, Xi'an Key Laboratory of Sustainable Energy and Materials Chemistry, Xi'an Jiaotong University, 99 Yanxiang Road, Xi'an, Shaanxi 710054, P. R. China.*

Corresponding email: hantian0123@xjtu.edu.cn; zheng.yanzhen@xjtu.edu.cn

Table of contents

1. General Experimental Section

Materials and methods. All reactions were carried out under a dry and oxygen-free argon atmosphere by using Schlenk techniques or in a glovebox. All solvents were dried and degassed by standard techniques. Anhydrous $DyCl_3$ salts were prepared according to the literature procedure.[1] $NaBH_4$, $NaBPh_4$, $[NEt_3H][Cl]$ (Triethylamine hydrochloride), 18-crown-6 ether are commercially available and were used without further treatment. $[NEt_3H][BPh_4]$ was obtained by the reaction of $[NEt_3H][Cl]$ with $NaBPh_4$.[2] Elemental analyses were performed on a EA3000 elemental analyser.

2. X-ray Crystallography Data

Single crystals suitable for X-ray analysis were coated with deoxygenated Paratone-N oil. All data were recorded on a Bruker Apex II diffractometer, equipped with CCD area detector and a graphite-monochromated MoKα radiation (λ = 0.71073 Å) at 250 K. The structures were solved by direct methods and refined by full-matrix least-squares methods on all unique F^2 values using SHELXTL.[3] The non-hydrogen atoms were determined from different Fourier maps and refined anisotropically. Hydrogen atoms were placed at calculated positions and refined with fixed geometry with respect to their carrier atoms in Olex2. CCDC 1968912 (**1**), 1968913 (**2**) and 1968915 (**3**) contains the supplementary crystallographic data for this paper. These data can be obtained free of charge via www.ccdc.cam.ac.uk/conts/retrieving.html (or from the Cambridge Crystallographic Data Centre, 12 Union Road, Cambridge CB21EZ, UK; fax: (+44)1223-336-033; or deposit@ccdc.cam.ac.uk).

Table S1. Crystallographic data for complexes **1**, **2** and **3**.

	1	**2**	**3**
Empirical formula	$DyC_{12}H_{36}B_3O_3$	$DyC_{44}H_{68}B_3O_5$	$DyC_{80}H_{112}B_4NaO_{14}$
Formula weight (g mol^{-1})	423.34	871.91	1526.42
Crystal system	Orthorhombic	Monoclinic	Monoclinic
Space group	*P*bcn	*P*2(1)/c	*P*2(1)/c
T (K)	250.15	250.15	250.15
a [Å]	9.2218(3)	13.651(3)	11.208(4)
b [Å]	14.4491(4)	13.265(3)	18.045(6)
c [Å]	14.5213(4)	24.810(6)	20.555(7)
α [°]	90	90	90
β [°]	90	90.453(3)	101.305(4)
γ [°]	90	90	90
V [Å^3]	1934.92(10)	4492.5(18)	4077(2)
Z	4	4	2
ρ_{calcd} [g cm^{-3}]	1.453	1.289	1.243
F (000)	852	1812	1602
Reflns collected	11515	53405	20977
Unique reflns	2248	7857	7925
R_{int}	0.0212	0.0373	0.0161
Parameters / restraints	112 / 22	498 / 110	446 / 47
GOF	1.139	1.218	1.104
R_1 [all data]	0.0349	0.0916	0.0467
R_1 [I>2sigma(I)]	0.0253	0.0879	0.0343
wR_2 (all data)	0.0833	0.2274	0.1084
wR_2 (I>2sigma(I))	0.0746	0.2253	0.0989
Largest diff. peak/hole [e Å^{-3}]	1.044 / -0.556	2.558 / -2.987	1.198 / -0.800

2.1 Selected distances and angles (deg) for complex 1

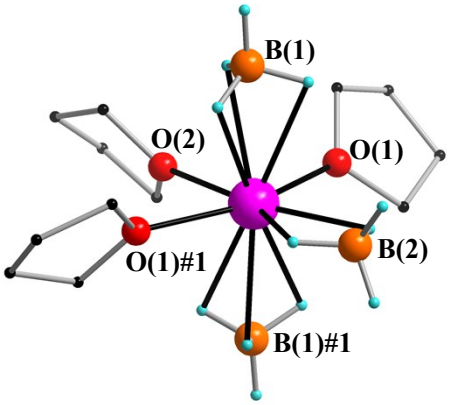

Figure S1. Crystal structure of complex **1**. Dy: fuschia, C: black, B: Orange, O: red, H: Aqua. Hydrogen atoms for THF are omitted for clarity.

Table S2. Selected distances (Å) in complex **1**.

Dy(1)-O(1)	2.348(3)	Dy(1)···B(1)	2.541(4)
Dy(1)-O(1)#1	2.348(3)	Dy(1)···B(1)#1	2.541(4)
Dy(1)-O(2)	2.418(4)	Dy(1)···B(2)	2.693(7)

Symmetry codes: #1 -x+1, y, -z+1/2

Table S3. Selected angles (deg) in complex **1**.

O(1)-Dy(1)-O(2)	78.80(8)	O(1)#1-Dy(1)-O(2)	78.80(8)
O(1)-Dy(1)-B(2)	101.20(8)	O(1)#1-Dy(1)-B(2)	101.20(8)
O(1)-Dy(1)-B(1)	88.92(12)	O(1)#1-Dy(1)-B(1)	90.11(12)
O(2)-Dy(1)-B(1)	87.49(10)	B(1)-Dy(1)-B(2)	92.51(10)
O(1)-Dy(1)-B(1)#1	90.11(12)	O(1)#1-Dy(1)-B(1)#1	88.91(12)
O(2)-Dy(1)-B(1)#1	87.49(10)	B(1)#1-Dy(1)-B(2)	92.51(10)
B(1)-Dy(1)-B(1)#1	174.97(19)		

Symmetry codes: #1 -x+1, y, -z+1/2

Table S4. Continuous Shape Measures Calculations for complex **1**.[4]

Structure [a]	HP-6	PPY-6	OC-6	TPR-6	JPPY-6
1	33.840	26.245	1.228	15.330	29.470

[a] HP-6, D_{6h}, Hexagon; PPY-6, C_{5v}, Pentagonal pyramid; OC-6, O_h, Octahedron; TPR-6, D_{3h}, Trigonal prism; JPPY-6, C_{5v}, Johnson pentagonal pyramid J2.

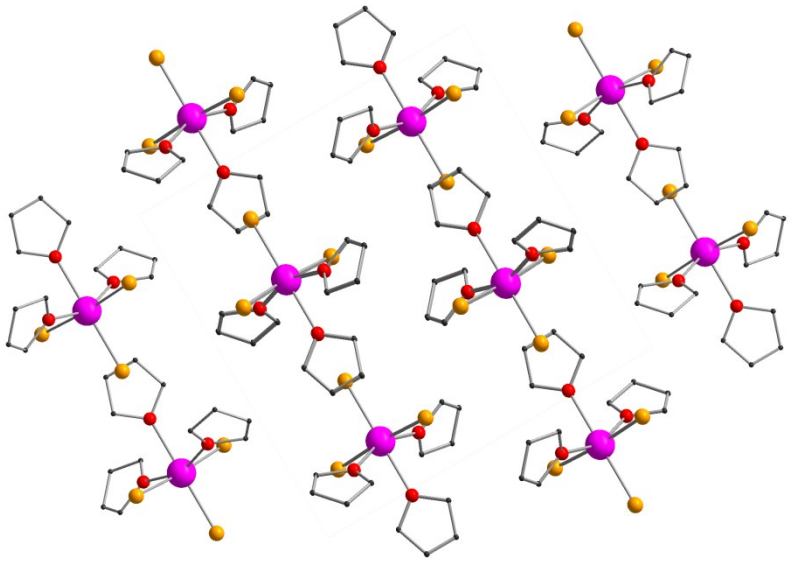

Figure S2. Packing diagram for complex **1** shown along the crystallographic *a* axis.

2.2 Selected distances and angles (deg) for complex 2

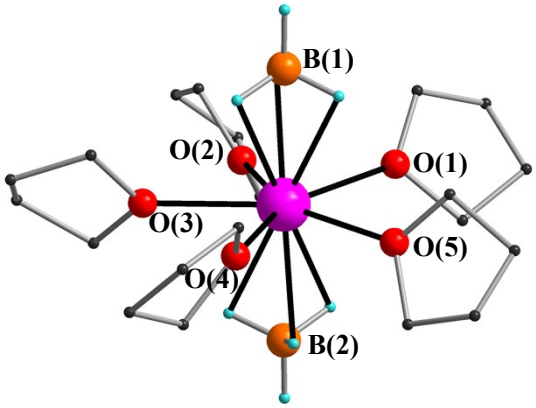

Figure S3. Crystal structure of the cation in complex **2.** Dy: fuschia, C: black, B: Orange, O: red, H: Aqua. Hydrogen atoms for THF are omitted for clarity.

Table S5. Selected distances (Å) in complex **2**.

Dy(1)-O(1)	2.443(10)	Dy(1)-O(2)	2.433(9)
Dy(1)-O(3)	2.431(8)	Dy(1)-O(4)	2.466(7)
Dy(1)-O(5)	2.423(9)		
Dy(1)···B(1)	2.529(9)	Dy(1)···B(2)	2.518(10)

Table S6. Selected angles (deg) in complex **2**.

O(2)-Dy(1)-O(1)	72.1(4)	O(1)-Dy(1)-B(1)	89.8(4)	O(1)-Dy(1)-B(2)	91.2(4)
O(5)-Dy(1)-O(1)	71.9(4)	O(2)-Dy(1)-B(1)	90.0(3)	O(2)-Dy(1)-B(2)	90.2(3)
O(3)-Dy(1)-O(2)	70.8(3)	O(3)-Dy(1)-B(1)	87.0(3)	O(3)-Dy(1)-B(2)	92.0(3)
O(3)-Dy(1)-O(4)	69.0(3)	O(4)-Dy(1)-B(1)	92.8(3)	O(4)-Dy(1)-B(2)	86.4(3)
O(5)-Dy(1)-O(4)	76.6(3)	O(5)-Dy(1)-B(1)	87.8(3)	O(5)-Dy(1)-B(2)	92.7(3)
B(2)-Dy(1)-B(1)	178.9(4)				

Table S7. Continuous Shape Measures Calculations for complex **2**.

Structure [a]	HP-7	HPY-7	PBPY-7	COC-7	CTPR-7	JPBPY-7	JETPY-7
2	34.343	26.012	0.165	7.380	5.610	4.372	23.876

[a] HP-7 D_{7h} Heptagon; HPY-7 C_{6v} Hexagonal pyramid; PBPY-7 D_{5h} Pentagonal bipyramid; COC-7 C_{3v} Capped octahedron; CTPR-7 C_{2v} Capped trigonal prism; JPBPY-7 D_{5h} Johnson pentagonal bipyramid J13; JETPY-7 C_{3v} Johnson elongated triangular pyramid J7

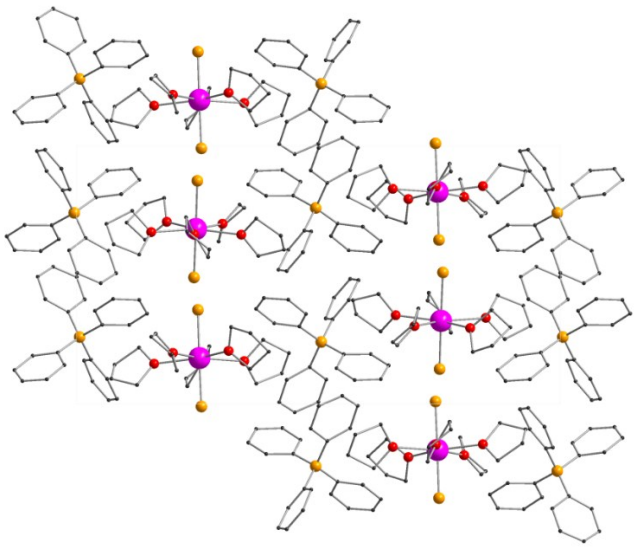

Figure S4. Packing diagram for complex **2** shown along the crystallographic *a* axis.

2.3 Selected distances and angles (deg) for complex 3

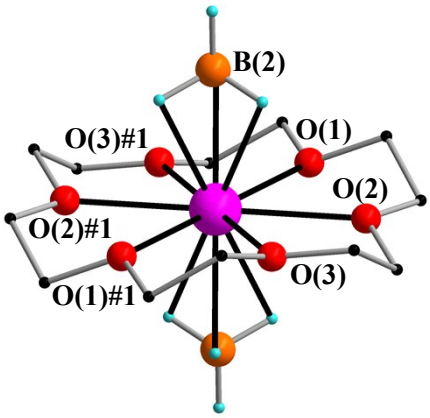

Figure S5. Crystal structure of the cation in complex **3.** Dy: fuschia, C: black, B: Orange, O: red, H: Aqua. Hydrogen atoms for 18-C-6 are omitted for clarity.

Table S8. Selected distances (Å) in complex **3**.

Dy(1)-O(1)	2.557(2)	Dy(1)-O(1)#1	2.557(2)
Dy(1)-O(2)	2.580(2)	Dy(1)-O(2)#1	2.580(2)
Dy(1)-O(3)	2.612(2)	Dy(1)-O(3)#1	2.612(2)
Dy(1)···B(2)	2.531(3)	Dy(1)···B(2)#1	2.531(3)

Symmetry codes: #1 -x+1, -y+1, -z+1

Table S9. Selected angles (deg) in complex **3**.

O(1)-Dy(1)-O(2)	60.73(8)	O(1)#1-Dy(1)-O(2)	119.27(8)
O(1)-Dy(1)-O(2)#1	119.27(8)	O(1)#1-Dy(1)-O(2)#1	60.73(8)
O(1)-Dy(1)-O(3)	120.07(8)	O(1)#1-Dy(1)-O(3)	59.93(8)
O(1)-Dy(1)-O(3)#1	59.93(8)	O(1)#1-Dy(1)-O(3)#1	120.07(8)
O(2)-Dy(1)-O(3)	59.47(8)	O(2)-Dy(1)-O(3)#1	120.53(8)
O(2)#1-Dy(1)-O(3)	120.53(8)	O(2)#1-Dy(1)-O(3)#1	59.47(8)
B(2)-Dy(1)-O(1)	91.43(10)	B(2)-Dy(1)-O(1)#1	88.57(10)
B(2)#1-Dy(1)-O(1)	88.57(10)	B(2)#1-Dy(1)-O(1)#1	91.43(10)
B(2)-Dy(1)-O(2)	88.88(11)	B(2)-Dy(1)-O(2)#1	91.11(11)
B(2)#1-Dy(1)-O(2)	91.12(11)	B(2)#1-Dy(1)-O(2)#1	88.88(11)
B(2)-Dy(1)-O(3)	91.09(11)	B(2)-Dy(1)-O(3)#1	88.91(11)
B(2)#1-Dy(1)-O(3)	88.91(11)	B(2)#1-Dy(1)-O(3)#1	91.09(11)
B(2)-Dy(1)-B(2)#1	180.00(14)		

Symmetry codes: #1 -x+1, -y+1, -z+1

Table S10. Continuous Shape Measures Calculations for complex **3**.

Structure [a]	OP-8	HPY-8	HBPY-8	CU-8	SAPR-8	TDD-8	JGBF-8
3	31.949	23.331	0.049	7.462	17.596	14.798	10.747
Structure [a]	JSD-8	TT-8	BTPR-8	ETBPY-8	JETBPY-8		JBTPR-8
3	18.722	8.337	17.003	23.202	26.091		17.699

[a] OP-8 D_{8h} Octagon; HPY-8 C_{7v} Heptagonal pyramid; HBPY-8 D_{6h} Hexagonal bipyramid; CU-8 O_h Cube; SAPR-8 D_{4d} Square antiprism; TDD-8 D_{2d} Triangular dodecahedron; JGBF-8 D_{2d} Johnson gyrobifastigium J26; JETBPY-8 D_{3h} Johnson elongated triangular bipyramid J14; JBTPR-8 C_{2v}Biaugmented trigonal prism J50; BTPR-8 C_{2v}Biaugmented trigonal prism; JSD-8 D_{2d} Snub diphenoid J84; TT-8 T_d Triakis tetrahedron; ETBPY-8 D_{3h} Elongated trigonal bipyramid

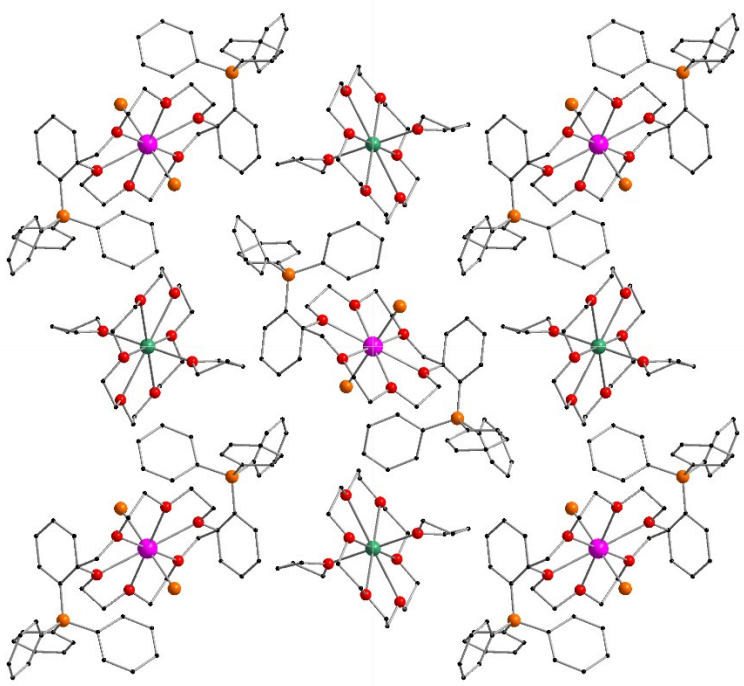

Figure S6. Packing diagram for complex **3** shown along the crystallographic *a* axis.

3. Magnetic Properties

Magnetic susceptibility measurements have been carried out with a Quantum Design MPMS-XL7 SQUID magnetometer upon cooling from 300 to 2 K in variable applied fields. Ac susceptibility measurements have been performed at frequencies of between 1 and 1500 Hz with an ac field of 3.5 Oe and with variable dc applied field. Powder samples were embedded in eicosane to avoid any field induced crystal reorientation. A diamagnetic correction has been calculated from Pascal constants and embedding eicosane has been applied to the observed magnetic susceptibility.

3.1 The magnetization dynamics for complex **1**.

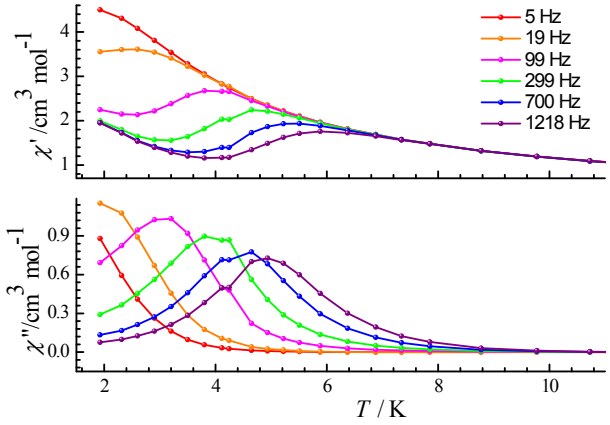

Figure S7. Temperature-dependence of in-phase (χ') and out-of-phase (χ'') magnetic susceptibility of **1** in an applied dc field of 500 Oe.

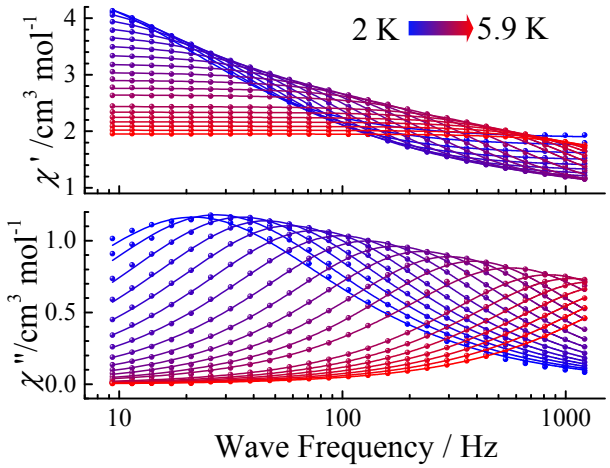

Figure S8. Frequency-dependence of χ' and χ'' magnetic susceptibility under 500 Oe dc field at temperatures from 2.0 K (blue) to 5.9 K (red) for **1**. The solid lines are best fits.

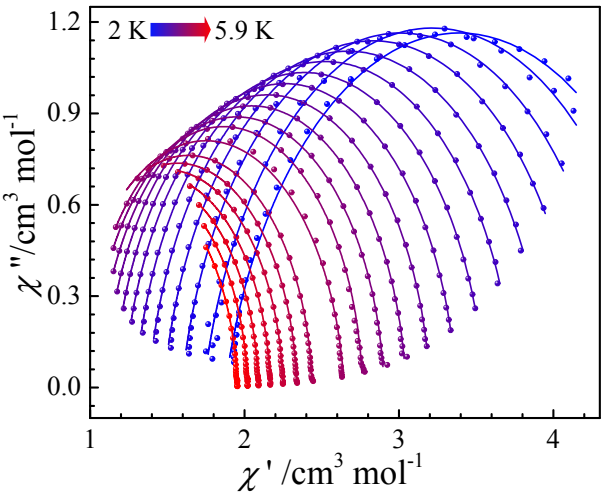

Figure S9. Cole-Cole plots at 500 Oe dc field for **1**. The solid lines are the best fits obtained with a generalized Debye model, with α parameters less than 0.17.

Table S11. Relaxation fitting parameters of a generalized Debye model for **1**.

T	χ_S	χ_T	τ	α
2.0	1.8739	4.90365	0.00739	0.16569
2.2	1.73425	4.69898	0.00584	0.14369
2.4	1.59095	4.43191	0.00449	0.12586
2.6	1.47525	4.18961	0.00351	0.1113
2.8	1.37625	3.96161	0.00274	0.09976
3.0	1.29221	3.75139	0.00212	0.08798
3.2	1.21761	3.55571	0.00163	0.07776
3.4	1.15281	3.37065	0.00124	0.06711
3.6	1.09475	3.20032	9.31769E-4	0.05797
3.8	1.04251	3.04521	7.02117E-4	0.05049
4.0	0.99420	2.90329	5.30289E-4	0.04553
4.2	0.96396	2.76324	4.09573E-4	0.03114
4.4	0.85541	2.64394	2.82395E-4	0.06263
4.7	0.83465	2.43697	1.89486E-4	0.03167
4.9	0.79963	2.33743	1.49981E-4	0.02726
5.1	0.75996	2.24812	1.19316E-4	0.02626
5.3	0.72385	2.16575	9.63145E-5	0.0249
5.5	0.67336	2.08919	7.71380E-5	0.02552
5.7	0.61302	2.01887	6.16958E-5	0.02752
5.9	0.53015	1.95233	4.85971E-5	0.03003

3.2 The magnetization dynamics for complex 3.

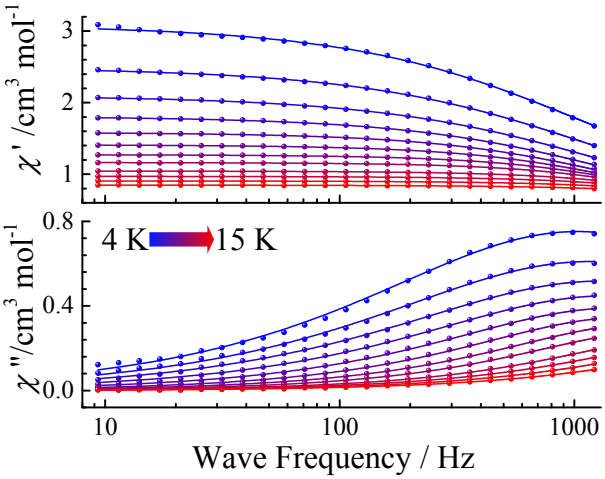

Figure S10. Frequency-dependence of χ' and χ'' magnetic susceptibility under zero dc field at temperatures from 4 K (blue) to 15 K (red) for **3**. The solid lines are the best fits.

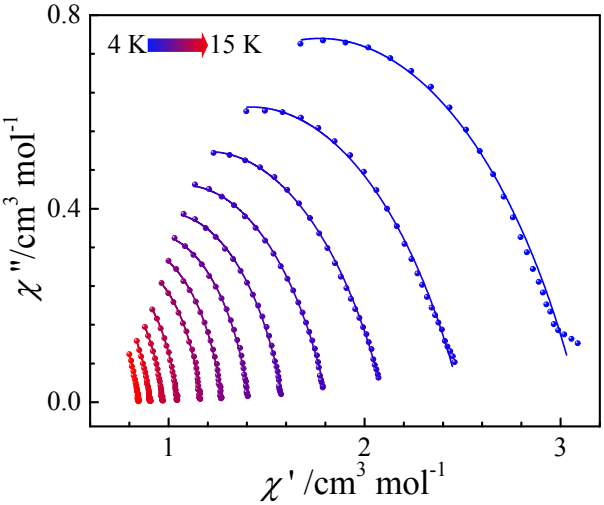

Figure S11. Cole-Cole plots at zero dc field for **3**. The solid lines are the best fits obtained with a generalized Debye model, with α parameters less than 0.34.

Table S12. Relaxation Fitting Parameters of a generalized Debye model for **3**.

T	χ_S	χ_T	τ	α
4	0.44948	3.09355	1.53951E-4	0.34158
5	0.34261	2.49574	1.36409E-4	0.34352
6	0.30137	2.1026	1.2094E-4	0.33549
7	0.34785	1.80994	1.12818E-4	0.29968
8	0.415	1.58586	1.06202E-4	0.25199
9	0.4456	1.41156	9.43608E-5	0.20773
10	0.42296	1.27348	7.52417E-5	0.18469
11	0.43255	1.16402	6.46181E-5	0.15968
12	0.35797	1.04496	4.28244E-5	0.16319
13	0.28848	0.97082	3.01359E-5	0.17448
14	0.28668	0.90657	2.44311E-5	0.1788
15	0.11044	0.84851	1.30359E-5	0.2021

4. Electronic Structure Calculations

Ab initio calculations at SA-CASSCF/RASSI level were performed on program MOLCAS 8.0[5] and the structure was originally taken from the X-Ray structure. The basis sets were chosen from the ANO-RCC library[6] as have been used in many works.[7,8] The Dy atom was treated with VTZP quality, then the related B, C and O atoms with VDZP quality and others with VDZ quality. The state-averaged CASSCF orbitals of the sextets, quartets and doublets were optimized with 21, 224 and 490 states, respectively, with the RASSCF module. 21, 128 and 130 sextets, quartets and doublets chosen to construct and diagonalize in spin-orbit (SO) coupling Hamiltonian with the RASSI[9] module. These computed SO states were written into the SINGLE_ANISO[10] program to compute the g-tensors, crystal field parameters and magnetic energy levels for the doublets of the ground $J = 15/2$ multiple of the $^6H_{15/2}$ term for Dy(III). The two electron integrals were Cholesky decomposed with a threshold of 1×10^{-8} to account for the accuracy.[11]

4.1 SA-CASSCF/RASSI calculated electronic states for complexes 1–3.

Table S13. SA-CASSCF/RASSI calculated electronic states for **1**.

Energy (cm^{-1})	Energy (K)	g_x	g_y	g_z	g_z Angle (°)	Wavefunction
0	0	0.00	0.00	18.29	--	80%$\vert \pm 15/2\rangle$
50	72	0.86	4.74	14.90	90	15%$\vert \pm 5/2\rangle$ + 23%$\vert \pm 3/2\rangle$ + 31%$\vert \mp 1/2\rangle$ + 12%$\vert \mp 3/2\rangle$
76	109	1.13	2.01	15.79	90	10%$\vert \pm 9/2\rangle$ + 13%$\vert \pm 3/2\rangle$ + 36%$\vert \pm 1/2\rangle$ + 14%$\vert \mp 3/2\rangle$
114	164	2.26	2.74	13.77	86	36%$\vert \pm 5/2\rangle$ + 13%$\vert \mp 3/2\rangle$ + 10%$\vert \mp 5/2\rangle$
174	250	9.11	5.53	0.08	62	48%$\vert \pm 5/2\rangle$
223	321	9.14	6.05	2.46	90	45%$\vert \pm 9/2\rangle$ + 13%$\vert \pm 7/2\rangle$
273	392	2.08	2.35	15.19	25	68%$\vert \pm 13/2\rangle$ + 10%$\vert \pm 5/2\rangle$
287	413	0.26	2.59	14.58	24	57%$\vert \pm 11/2\rangle$ + 14%$\vert \pm 9/2\rangle$ + 11%$\vert \mp 11/2\rangle$

[a] Only components with > 10% contribution are given, rounded to the nearest percent.

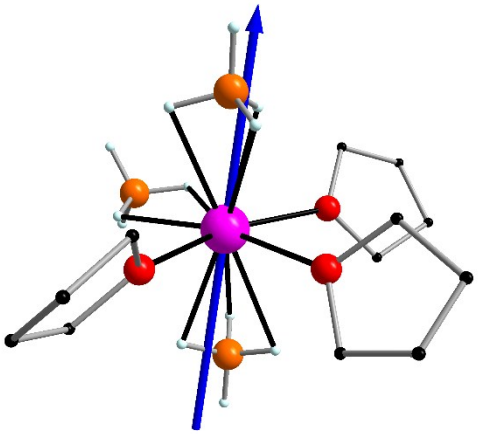

Figure S12. The principal magnetic axis of the ground Kramer's doublet of **1**.

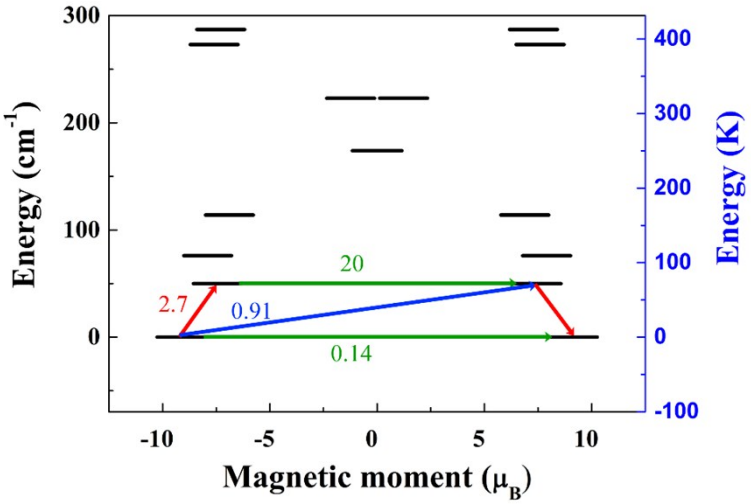

Figure S13. *Ab initio* calculated electronic states of the $J = 15/2$ manifold of the $^6H_{15/2}$ term of Dy^{III} in **1**.

Table S14. SA-CASSCF/RASSI calculated electronic states for **2**.

Energy (cm^{-1})	Energy (K)	g_x	g_y	g_z	g_z Angle (°)	Wavefunction
0	0	0.00	0.00	15.81	-	17%| ± 15/2> + 12%| ± 5/2> + 19%| ± 3/2> + 23%| ± 1/2> + 11%| ∓ 1/2>
8	12	0.10	0.90	14.81	57	69%| ± 15/2>
28	40	0.84	1.38	14.24	26	11%| ± 5/2> + 42%| ± 3/2> + 13%| ± 1/2> + 22%| ∓ 5/2>
56	80	1.31	2.40	12.91	68	16%| ± 7/2> + 32%| ± 5/2> + 11%| ∓ 3/2> + 12%| ∓ 7/2>
86	124	4.52	5.72	7.57	75	35%| ± 7/2> + 11%| ± 3/2> + 12%| ∓ 1/2> + 17%| ∓ 7/2>
151	217	0.97	1.30	11.84	71	79%| ± 9/2>
228	328	0.15	0.28	15.45	77	92%| ± 11/2>
249	358	0.06	0.08	17.57	65	93%| ± 13/2>

[a] Only components with > 10% contribution are given, rounded to the nearest percent.

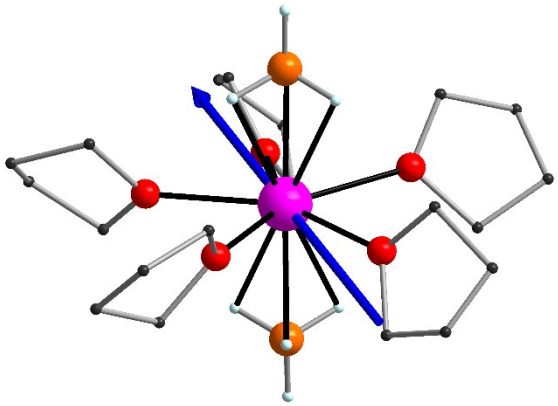

Figure S14. The principal magnetic axis of the ground Kramer's doublet of **2**.

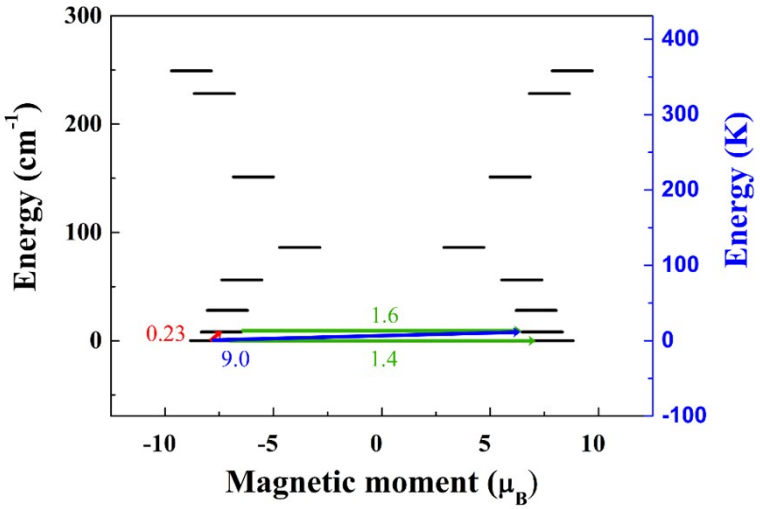

Figure S15. *Ab initio* calculated electronic states of the $J = 15/2$ manifold of the $^6H_{15/2}$ term of Dy^{III} in **2**.

Table S15. SA-CASSCF/RASSI calculated electronic states for **3**.

Energy (cm^{-1})	Energy (K)	g_x	g_y	g_z	g_z Angle (°)	Wavefunction
0	0	0.00	0.00	19.84	-	99%| ± 15/2>
250	359	1.94	2.97	15.13	5.9	85%| ± 13/2>
285	410	0.22	1.63	15.89	73	11%| ± 11/2> + 14%| ± 9/2> + 19%| ± 7/2> + 15%| ∓ 5/2>
307	441	10.27	7.19	2.31	33	23%| ± 11/2> + 19%| ± 9/2> + 13%| ∓ 3/2> + 10%| ∓ 9/2>
330	475	0.03	1.76	14.16	66	18%| ± 11/2> + 10%| ± 9/2> + 10%| ± 3/2> + 10%| ∓ 7/2> + 18%| ∓ 11/2>
392	564	0.45	2.03	15.78	88	16%| ± 11/2> + 19%| ± 5/2> + 20%| ∓ 1/2> + 10%| ∓ 7/2> + 10%| ∓ 9/2>
423	608	0.79	1.14	17.02	88	11%| ± 9/2> + 23%| ± 3/2> + 20%| ∓ 1/2> + 10%| ∓ 3/2> + 10%| ∓ 5/2>
459	660	0.08	0.49	18.42	87	12%| ± 5/2> + 15%| ± 1/2> + 15%| ∓ 1/2> + 13%| ∓ 3/2> + 10%| ∓ 7/2>

[a] Only components with > 10% contribution are given, rounded to the nearest percent.

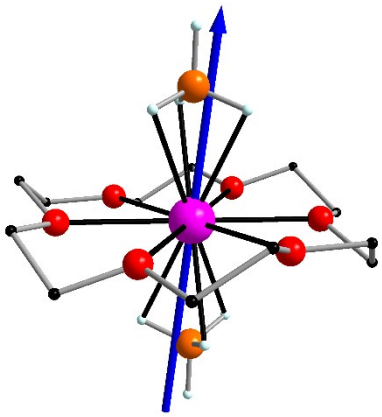

Figure S16. The principal magnetic axis of the ground Kramer's doublet of **3**.

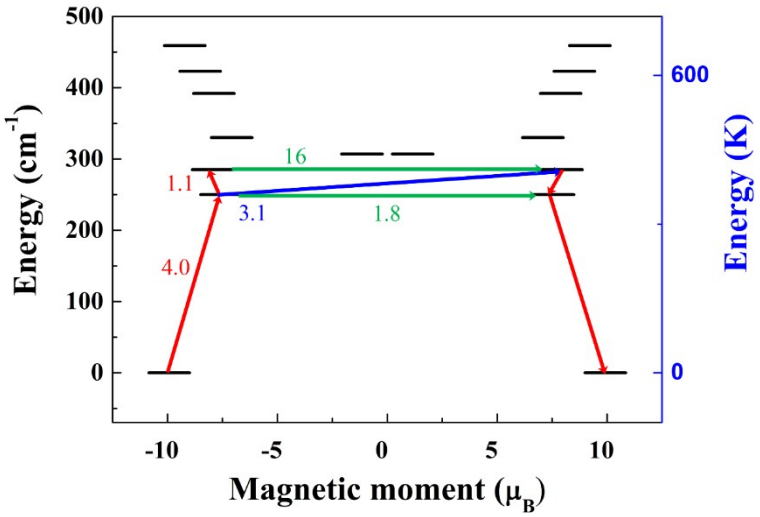

Figure S17. *Ab initio* calculated electronic states of the $J = 15/2$ manifold of the $^6H_{15/2}$ term of Dy^{III} in **3**.

Table S16. CASSCF computed LoProp charges of the atoms attached to the Dy center.

Atom label	**1**	Atom label	**2**	Atom label	**3**
Dy(1)	2.6215	Dy(1)	2.6060	Dy(1)	2.5991
O(1)	-0.5691	B(1)	-0.7728	B(2)	-0.7825
O(1)#1	-0.5691	B(2)	-0.7688	B(2)#1	-0.7825
O(2)	-0.5406	O(1)	-0.5411	O(1)	-0.5247
B(1)	-0.7711	O(2)	-0.5739	O(1)#1	-0.5247
B(1)#1	-0.7711	O(3)	-0.5595	O(2)	-0.5152
B(2)	-0.6718	O(4)	-0.5621	O(2)#1	-0.5142
		O(5)	-0.5626	O(3)	-0.5142
				O(3)#1	-0.5142

4.2 *Ab initio* calculated crystal field parameters for complexes 1-3.

Table S17. *Ab initio* calculated crystal field parameters for **1**.

Crystal Field Parameter	Value / cm^{-1}
B_2^{-2}	0.10600140887493E-03
B_2^{-1}	-0.38582572072175E-01
B_2^0	0.81347184292867E-01
B_2^1	-0.28727179237197E-04
B_2^2	0.12355818898048E+00
B_4^{-4}	-0.27667121560857E-04
B_4^{-3}	-0.14670583301043E-01
B_4^{-2}	0.94329720711812E-06
B_4^{-1}	-0.11869479514889E-01
B_4^0	-0.62311382538965E-02
B_4^1	-0.14462578809407E-05
B_4^2	0.31136782914248E-02
B_4^3	0.15005568379797E-04
B_4^4	-0.28469985652337E-01
B_6^{-6}	-0.18358724994441E-06
B_6^{-5}	-0.23446832660325E-03
B_6^{-4}	-0.20227631661079E-06
B_6^{-3}	0.61475844135920E-04
B_6^{-2}	-0.40465439191611E-07
B_6^{-1}	-0.33418907263503E-03
B_6^0	-0.26987535618516E-04
B_6^1	0.45461469636182E-07
B_6^2	-0.18544880737566E-04
B_6^3	-0.96042958520923E-08
B_6^4	-0.21785434534274E-03
B_6^5	0.22869582594439E-06
B_6^6	-0.12400032235547E-03

Table S18. *Ab initio* calculated crystal field parameters for **2**.

Crystal Field Parameter	Value / cm^{-1}
B_2^{-2}	0.25826180843177E-01
B_2^{-1}	-0.16980740311182E+00
B_2^0	0.59081886662883E+00
B_2^1	0.24999914711416E-01
B_2^2	-0.44626265327969E+00
B_4^{-4}	0.17137346854433E-02
B_4^{-3}	0.16543976486808E-03
B_4^{-2}	0.10009442877224E-02
B_4^{-1}	-0.11854151594280E-01
B_4^0	-0.62057122300117E-02
B_4^1	0.50138658343808E-02
B_4^2	0.25939623611562E-02
B_4^3	-0.47741895110092E-02
B_4^4	0.20945353762627E-02
B_6^{-6}	-0.20464716194620E-04
B_6^{-5}	0.30369281618911E-03
B_6^{-4}	0.30972663618880E-04
B_6^{-3}	0.22797181594451E-03
B_6^{-2}	0.67568934909863E-04
B_6^{-1}	-0.17535268331091E-03
B_6^0	-0.39562543244306E-04
B_6^1	0.51524887718694E-04
B_6^2	0.81428654287264E-05
B_6^3	0.20374572677152E-03
B_6^4	-0.54185345877737E-04
B_6^5	-0.16644361941474E-03
B_6^6	0.27701874475471E-04

Table S19. *Ab initio* calculated crystal field parameters for **3**.

Crystal Field Parameter	Value / cm^{-1}
B_2^{-2}	0.16620117262922E-01
B_2^{-1}	0.11605866427043E-02
B_2^0	-0.18754401789672E+01
B_2^1	-0.27630633707479E-01
B_2^2	0.47341039234922E+00
B_4^{-4}	0.33480466705950E-02
B_4^{-3}	0.10285966408991E-01
B_4^{-2}	0.18873757854725E-02
B_4^{-1}	0.37062931300344E-02
B_4^0	-0.49167094129449E-02
B_4^1	0.96042627298236E-03
B_4^2	-0.59224934154481E-03
B_4^3	-0.20487227496936E-01
B_4^4	0.17438347250430E-02
B_6^{-6}	0.48491940603878E-03
B_6^{-5}	0.35699029529318E-04
B_6^{-4}	0.24098878165368E-04
B_6^{-3}	-0.24550818185986E-03
B_6^{-2}	-0.44505133259917E-04
B_6^{-1}	0.67832348397534E-04
B_6^0	-0.28834289517000E-04
B_6^1	0.59590694470317E-04
B_6^2	-0.25243815094198E-04
B_6^3	0.64595654068746E-05
B_6^4	-0.11599984146356E-04
B_6^5	0.15436993553348E-03
B_6^6	0.18123120358621E-03

Table S20. Average transition magnetic moment elements between the states of **1**, given in μ_B^2.

	$\left\|+\frac{15}{2}\right>$	$\left\|-\frac{15}{2}\right>$	$\left\|+\frac{13}{2}\right>$	$\left\|-\frac{13}{2}\right>$	$\left\|+\frac{11}{2}\right>$	$\left\|-\frac{11}{2}\right>$	|+a>	|-a>	|+b>	|-b>	|+c>	|-c>	|+d>	|-d>	|+e>	|-e>
$\left\|+\frac{15}{2}\right>$	--	1.4E-01	2.7E+00	9.1E-01	8.9E-01	3.2E-01	9.1E-01	1.4E-01	3.3E-01	1.4E-01	3.5E-02	5.2E-01	1.3E+00	1.3E-01	3.5E-02	9.4E-01
$\left\|-\frac{15}{2}\right>$	1.4E-01	--	9.1E-01	2.7E+00	3.2E-01	8.9E-01	1.4E-01	9.1E-01	1.4E-01	3.3E-01	5.2E-01	3.5E-02	1.3E-01	1.3E+00	9.4E-01	3.5E-02
$\left\|+\frac{13}{2}\right>$	2.7E+00	9.1E-01	--	2.0E+01	5.0E+00	2.0E+00	2.7E+00	5.1E-01	1.2E+00	7.1E-01	3.0E-01	8.0E-02	2.0E-01	1.0E-01	9.7E-02	2.3E-01
$\left\|-\frac{13}{2}\right>$	9.1E-01	2.7E+00	2.0E+01	--	2.0E+00	5.0E+00	5.1E-01	2.7E+00	7.1E-01	1.2E+00	8.0E-02	3.0E-01	1.0E-01	2.0E-01	2.3E-01	9.7E-02
$\left\|+\frac{11}{2}\right>$	8.9E-01	3.2E-01	5.0E+00	2.0E+00	--	1.4E+01	3.8E+00	1.2E+00	5.5E-01	1.5E+00	1.4E-01	1.6E-01	2.5E-01	8.8E-02	3.0E-03	1.6E-01
$\left\|-\frac{11}{2}\right>$	3.2E-01	8.9E-01	2.0E+00	5.0E+00	1.4E+01	--	1.2E+00	3.8E+00	1.5E+00	5.5E-01	1.6E-01	1.4E-01	8.8E-02	2.5E-01	1.6E-01	3.0E-03
|+a>	9.1E-01	1.4E-01	2.7E+00	5.1E-01	3.8E+00	1.2E+00	--	1.3E+01	2.0E+00	6.0E+00	9.1E-01	1.6E+00	4.7E-01	4.5E-01	2.3E-01	1.0E-01
|-a>	1.4E-01	9.1E-01	5.1E-01	2.7E+00	1.2E+00	3.8E+00	1.3E+01	--	6.0E+00	2.0E+00	1.6E+00	9.1E-01	4.5E-01	4.7E-01	1.0E-01	2.3E-01
|+b>	3.3E-01	1.4E-01	1.2E+00	7.1E-01	5.5E-01	1.5E+00	2.0E+00	6.0E+00	--	8.1E+00	7.8E+00	3.4E+00	1.0E+00	2.4E+00	5.5E-01	2.3E-01
|-b>	1.4E-01	3.3E-01	7.1E-01	1.2E+00	1.5E+00	5.5E-01	6.0E+00	2.0E+00	8.1E+00	--	3.4E+00	7.8E+00	2.4E+00	1.0E+00	2.3E-01	5.5E-01
|+c>	3.5E-02	5.2E-01	3.0E-01	8.0E-02	1.4E-01	1.6E-01	9.1E-01	1.6E+00	7.8E+00	3.4E+00	--	7.2E+00	8.9E-01	2.9E+00	6.4E+00	1.9E+00

|-c>	5.2E-01	3.5E-02	8.0E-02	3.0E-01	1.6E-01	1.4E-01	1.6E+00	9.1E-01	3.4E+00	7.8E+00	7.2E+00	--	2.9E+00	8.9E-01	1.9E+00	6.4E+00
|+d>	1.3E+00	1.3E-01	2.0E-01	1.0E-01	2.5E-01	8.8E-02	4.7E-01	4.5E-01	1.0E+00	2.4E+00	8.9E-01	2.9E+00	--	3.1E+00	3.6E+00	3.3E+00
|-d>	1.3E-01	1.3E+00	1.0E-01	2.0E-01	8.8E-02	2.5E-01	4.5E-01	4.7E-01	2.4E+00	1.0E+00	2.9E+00	8.9E-01	3.1E+00	--	3.3E+00	3.6E+00
|+e>	3.5E-02	9.4E-01	9.7E-02	2.3E-01	3.0E-03	1.6E-01	2.3E-01	1.0E-01	5.5E-01	2.3E-01	6.4E+00	1.9E+00	3.6E+00	3.3E+00	--	6.1E+00
|-e>	9.4E-01	3.5E-02	2.3E-01	9.7E-02	1.6E-01	3.0E-03	1.0E-01	2.3E-01	2.3E-01	5.5E-01	1.9E+00	6.4E+00	3.3E+00	3.6E+00	6.1E+00	--

Table S21. Average transition magnetic moment elements between the states of **2**, given in μ_B^2.

	$\lvert+\frac{15}{2}\rangle$	$\lvert-\frac{15}{2}\rangle$	$\lvert+\frac{13}{2}\rangle$	$\lvert-\frac{13}{2}\rangle$	$\lvert+\frac{11}{2}\rangle$	$\lvert-\frac{11}{2}\rangle$	$\lvert+a\rangle$	$\lvert-a\rangle$	$\lvert+b\rangle$	$\lvert-b\rangle$	$\lvert+c\rangle$	$\lvert-c\rangle$	$\lvert+d\rangle$	$\lvert-d\rangle$	$\lvert+e\rangle$	$\lvert-e\rangle$
$\lvert+\frac{15}{2}\rangle$	--	1.4E+00	2.3E-01	9.0E+00	1.8E+00	2.8E+00	5.9E-01	5.6E-01	1.7E-01	4.2E-01	1.9E-01	1.6E-01	3.1E-01	1.8E-02	2.6E-03	5.9E-01
$\lvert-\frac{15}{2}\rangle$	1.4E+00	--	9.0E+00	2.3E-01	2.8E+00	1.8E+00	5.6E-01	5.9E-01	4.2E-01	1.7E-01	1.6E-01	1.9E-01	1.8E-02	3.1E-01	5.9E-01	2.6E-03
$\lvert+\frac{13}{2}\rangle$	2.3E-01	9.0E+00	--	1.6E+00	3.8E-01	8.5E-01	5.6E-01	3.3E-01	3.9E-01	5.4E-01	1.1E-01	1.1E-01	2.4E-02	5.8E-01	2.6E+00	1.5E-03
$\lvert-\frac{13}{2}\rangle$	9.0E+00	2.3E-01	1.6E+00	--	8.5E-01	3.8E+00	3.3E-01	5.6E-01	5.4E-01	3.9E-01	1.1E-01	1.1E-01	5.8E-01	2.4E-02	1.5E-03	2.6E+00
$\lvert+\frac{11}{2}\rangle$	1.8E+00	2.8E+00	3.8E-01	8.5E-01	--	8.6E+00	4.6E+00	2.4E+00	2.2E+00	1.1E+00	2.8E-01	3.4E-01	1.0E-01	5.3E-02	2.3E-01	1.9E-02
$\lvert-\frac{11}{2}\rangle$	2.8E+00	1.8E+00	8.5E-01	3.8E+00	8.6E+00	--	2.4E+00	4.6E+00	1.1E+00	2.2E+00	3.4E-01	2.8E-01	5.3E-02	1.0E-01	1.9E-02	2.3E-01
$\lvert+a\rangle$	5.9E-01	5.6E-01	5.6E-01	3.3E-01	4.6E+00	2.4E+00	--	1.3E+01	6.2E+00	5.9E+00	1.3E+00	3.9E-01	3.2E-02	4.4E-02	2.1E-01	5.2E-02
$\lvert-a\rangle$	5.6E-01	5.9E-01	3.3E-01	5.6E-01	2.4E+00	4.6E+00	1.3E+01	--	5.9E+00	6.2E+00	3.9E-01	1.3E+00	4.4E-02	3.2E-02	5.2E-02	2.1E-01
$\lvert+b\rangle$	1.7E-01	4.2E-01	3.9E-01	5.4E-01	2.2E+00	1.1E+00	6.2E+00	5.9E+00	--	7.1E+00	6.5E+00	5.0E+00	1.6E-01	5.1E-02	9.4E-02	2.6E-02
$\lvert-b\rangle$	4.2E-01	1.7E-01	5.4E-01	3.9E-01	1.1E+00	2.2E+00	5.9E+00	6.2E+00	7.1E+00	--	5.0E+00	6.5E+00	5.1E-02	1.6E-01	2.6E-02	9.4E-02
$\lvert+c\rangle$	1.9E-01	1.6E-01	1.1E-01	1.1E-01	2.8E-01	3.4E-01	1.3E+00	3.9E-01	6.5E+00	5.0E+00	--	2.4E-01	1.0E+01	3.5E-02	1.9E-03	1.1E+00

|-c>	1.6E-01	1.9E-01	1.1E-01	1.1E-01	3.4E-01	2.8E-01	3.9E-01	1.3E+00	5.0E+00	6.5E+00	2.4E-01	--	3.5E-02	1.0E+01	1.1E+00	1.9E-03
|+d>	3.1E-01	1.8E-02	2.4E-02	5.8E-01	1.0E-01	5.3E-02	3.2E-02	4.4E-02	1.6E-01	5.1E-02	1.0E+01	3.5E-02	--	7.4E-02	6.2E-03	7.0E+00
|-d>	1.8E-02	3.1E-01	5.8E-01	2.4E-02	5.3E-02	1.0E-01	4.4E-02	3.2E-02	5.1E-02	1.6E-01	3.5E-02	1.0E+01	7.4E-02	--	7.0E+00	6.2E-03
|+e>	2.6E-03	5.9E-01	2.6E+00	1.5E-03	2.3E-01	1.9E-02	2.1E-01	5.2E-02	9.4E-02	2.6E-02	1.9E-03	1.1E+00	6.2E-03	7.0E+00	--	8.8E-04
|-e>	5.9E-01	2.6E-03	1.5E-03	2.6E+00	1.9E-02	2.3E-01	5.2E-02	2.1E-01	2.6E-02	9.4E-02	1.1E+00	1.9E-03	7.0E+00	6.2E-03	8.8E-04	--

Table S22. Average transition magnetic moment elements between the states of **3**, given in μ_B^2.

	$\left\|+\frac{15}{2}\right>$	$\left\|-\frac{15}{2}\right>$	$\left\|+\frac{13}{2}\right>$	$\left\|-\frac{13}{2}\right>$	$\left\|+\frac{11}{2}\right>$	$\left\|-\frac{11}{2}\right>$	$\|+a\rangle$	$\|-a\rangle$	$\|+b\rangle$	$\|-b\rangle$	$\|+c\rangle$	$\|-c\rangle$	$\|+d\rangle$	$\|-d\rangle$	$\|+e\rangle$	$\|-e\rangle$
$\left\|+\frac{15}{2}\right>$	--	6.4E-06	1.8E-02	4.0E+00	1.6E-01	3.0E-02	6.6E-02	4.1E-02	1.2E-01	7.7E-02	2.2E-02	1.4E-02	1.4E-02	5.4E-03	4.2E-03	1.7E-02
$\left\|-\frac{15}{2}\right>$	6.4E-06	--	4.0E+00	1.8E-02	3.0E-02	1.6E-01	4.1E-02	6.6E-02	7.7E-02	1.2E-01	1.4E-02	2.2E-02	5.4E-03	1.4E-02	1.7E-02	4.2E-03
$\left\|+\frac{13}{2}\right>$	1.8E-02	4.0E+00	--	1.8E+00	3.1E+00	1.1E+00	3.5E+00	1.3E+00	1.7E+00	1.7E+00	3.8E-01	5.0E-02	1.9E-01	8.1E-02	4.0E-02	1.4E-01
$\left\|-\frac{13}{2}\right>$	4.0E+00	1.8E-02	1.8E+00	--	1.1E+00	3.1E+00	1.3E+00	3.5E+00	1.7E+00	1.7E+00	5.0E-02	3.8E-01	8.1E-02	1.9E-01	1.4E-01	4.0E-02
$\left\|+\frac{11}{2}\right>$	1.6E-01	3.0E-02	3.1E+00	1.1E+00	--	1.6E+01	4.8E+00	1.1E+00	1.0E+00	7.3E-01	1.1E+00	1.5E+00	1.4E+00	7.9E-01	1.1E-01	1.0E-01
$\left\|-\frac{11}{2}\right>$	3.0E-02	1.6E-01	1.1E+00	3.1E+00	1.6E+01	--	1.1E+00	4.8E+00	7.3E-01	1.0E+00	1.5E+00	1.1E+00	7.9E-01	1.4E+00	1.0E-01	1.1E-01
$\|+a\rangle$	6.6E-02	4.1E-02	3.5E+00	1.3E+00	4.8E+00	1.1E+00	--	1.1E+01	3.4E+00	3.5E+00	1.2E+00	2.4E+00	5.3E-01	7.5E-01	4.2E-01	9.5E-01
$\|-a\rangle$	4.1E-02	6.6E-02	1.3E+00	3.5E+00	1.1E+00	4.8E+00	1.1E+01	--	3.5E+00	3.4E+00	2.4E+00	1.2E+00	7.5E-01	5.3E-01	9.5E-01	4.2E-01
$\|+b\rangle$	1.2E-01	7.7E-02	1.7E+00	1.7E+00	1.0E+00	7.3E-01	3.4E+00	3.5E+00	--	1.7E+01	1.1E+00	2.0E+00	6.5E-01	9.3E-01	1.6E+00	1.6E+00
$\|-b\rangle$	7.7E-02	1.2E-01	1.7E+00	1.7E+00	7.3E-01	1.0E+00	3.5E+00	3.4E+00	1.7E+01	--	2.0E+00	1.1E+00	9.3E-01	6.5E-01	1.6E+00	1.6E+00
$\|+c\rangle$	2.2E-02	1.4E-02	3.8E-01	5.0E-02	1.1E+00	1.5E+00	1.2E+00	2.4E+00	1.1E+00	2.0E+00	--	1.9E+01	1.2E+00	3.8E+00	1.1E+00	3.7E-01

$\|-c\rangle$	1.4E-02	2.2E-02	5.0E-02	3.8E-01	1.5E+00	1.1E+00	2.4E+00	1.2E+00	2.0E+00	1.1E+00	1.9E+01	--	3.8E+00	1.2E+00	3.7E-01	1.1E+00
$\|+d\rangle$	1.4E-02	5.4E-03	1.9E-01	8.1E-02	1.4E+00	7.9E-01	5.3E-01	7.5E-01	6.5E-01	9.3E-01	1.2E+00	3.8E+00	--	2.3E+01	1.8E+00	7.1E-01
$\|-d\rangle$	5.4E-03	1.4E-02	8.1E-02	1.9E-01	7.9E-01	1.4E+00	7.5E-01	5.3E-01	9.3E-01	6.5E-01	3.8E+00	1.2E+00	2.3E+01	--	7.1E-01	1.8E+00
$\|+e\rangle$	4.2E-03	1.7E-02	4.0E-02	1.4E-01	1.1E-01	1.0E-01	4.2E-01	9.5E-01	1.6E+00	1.6E+00	1.1E+00	3.7E-01	1.8E+00	7.1E-01	--	1.4E+00
$\|-e\rangle$	1.7E-02	4.2E-03	1.4E-01	4.0E-02	1.0E-01	1.1E-01	9.5E-01	4.2E-01	1.6E+00	1.6E+00	3.7E-01	1.1E+00	7.1E-01	1.8E+00	1.4E+00	--

5. References

1. J. B. Reed, B. S. Hopkins, L. F. Audrieth, P. W. Selwood, R. Ward and J. J. Dejongh, *Inorg. Syn. Volume I,* 1939, 28.
2. D. Robert, M. Kondracka and J. Okuda, *Dalton Trans.*, 2008, 2667.
3. (a) G. M Sheldrick, *Acta Cryst. A Found. Adv.*, 2008, **64**, 112; (b) G. M. Sheldrick, *Acta Cryst. A Found. Adv.*, 2015, **71**, 3; (c) G. M. Sheldrick, *Acta Cryst. C Struct. Chem.*, 2015, **71**, 3; (d) O. V. Dolomanov, L. J. Bourhis, R. J. Gildea, J. A. K. Howard and H. Puschmann, *J. Appl. Cryst.*, 2009, **42**, 339.
4. (a) S. Alvarez, D. Avnir, M. Llunell and M. Pinsky, *New J. Chem.*, 2002, **26**, 996; (b) D. Casanova, P. Alemany, J. M. Bofill and S. Alvarez, *Chem. Eur. J.*, 2003, **9**, 1281; (c) J. Cirera, P. Alemany and S. Alvarez, *Chem. Eur. J.*, 2004, **10**, 190; (d) D. Casanova, M. Llunell, P. Alemany and S. Alvarez, *Chem. Eur. J.*, 2005, **11**, 1479.
5. F. Aquilante, J. Autschbach, R. K. Carlson, L. F. Chibotaru, M. G. Delcey, L. De Vico, I. Fdez. Galván, N. Ferré, L. M. Frutos, L. Gagliardi, M. Garavelli, A. Giussani, C. E. Hoyer, G. Li Manni, H. Lischka, D. Ma, P. Å. Malmqvist, T. Müller, A. Nenov, M. Olivucci, T. B. Pedersen, D. Peng, F. Plasser, B. Pritchard, M. Reiher, I. Rivalta, I. Schapiro, J. Segarra-Martí, M. Stenrup, D. G. Truhlar, L. Ungur, A. Valentini, S. Vancoillie, V. Veryazov, V. P. Vysotskiy, O. Weingart, F. Zapata and R. Lindh, *J. Comput. Chem.*, 2016, **37**, 506.
6. B. O. Roos, R. Lindh, P.-Å. Malmqvist, V. Veryazov and P.-O. Widmark, *J. Phys. Chem. A*, 2004, **108**, 2851.
7. C. A. Goodwin, F. Ortu, D. Reta, N. F. Chilton and D. P. Mills, *Nature*, 2017, **548**, 439.
8. P. A. Malmqvist, B. O. Roos and B. Schimmelpfennig, *Chem. Phys. Lett*., 2002, **357**, 230.
9. B. O. Roos, R. Lindh, P.-Å. Malmqvist, V. Veryazov and P.-O. Widmark, *Chem. Phys. Lett*., 2005, **409**, 295.
10. (a) P. J. Stephens, F. J. Devlin, C. F. Chabalowski and M. J. Frisch, *J. Phys. Chem*., 1994, **98**, 11623; (b) A. D. Becke, *J. Chem. Phys*., 1993, **98**, 5648; (c) C. T. Lee, W. T. Yang and R. G. Parr, *Phys. Rev. B,* 1988, **37**, 785; (d) A. D. Becke, *Phys. Rev. A,* 1988, **38**, 3098.
11. T. R. Cundari and W. J. Stevens, *J. Chem. Phys*., 1993, **98**, 5555.